

Summer 2020

Spatiotemporal Dynamics of Benthic Microalgae in South Carolina Shelf Sediments

Sarah N. Zaunbrecher

Follow this and additional works at: <https://scholarcommons.sc.edu/etd>



Part of the [Marine Biology Commons](#)

Recommended Citation

Zaunbrecher, S. N. (2020). *Spatiotemporal Dynamics of Benthic Microalgae in South Carolina Shelf Sediments*. (Master's thesis). Retrieved from <https://scholarcommons.sc.edu/etd/6021>

This Open Access Thesis is brought to you by Scholar Commons. It has been accepted for inclusion in Theses and Dissertations by an authorized administrator of Scholar Commons. For more information, please contact digres@mailbox.sc.edu.

SPATIOTEMPORAL DYNAMICS OF BENTHIC MICROALGAE IN
SOUTH CAROLINA SHELF SEDIMENTS

by

Sarah N. Zaunbrecher

Bachelor of Science
Louisiana State University, 2015

Submitted in Partial Fulfillment of the Requirements

For the Degree of Masters of Science in

Marine Science

College of Arts and Sciences

University of South Carolina

2020

Accepted by:

James L. Pinckney, Director of Thesis

Ronald Benner, Reader

Susan Q. Lang, Reader

Cheryl L. Addy, Vice Provost and Dean of the Graduate School

© Copyright by Sarah N. Zaunbrecher, 2020
All Rights Reserved.

ACKNOWLEDGEMENTS

First and foremost, I'd like to thank my advisor, Dr. James L. Pinckney, whose invaluable guidance has helped me take this first big step in my scientific career. With his help, I have gained so many new skills and have begun to forge my own path as a scientist. Dr. Pinckney has helped me grow both professionally and personally and has been a caring and supportive mentor during these past two years. I could not have asked for a better advisor. I would also like to thank my committee members, Dr. Ronald Benner and Dr. Susan Q. Lang, for their guidance and expertise. Both have been patient and understanding during my time at USC, and they helped me to build my confidence as a researcher while simultaneously teaching me and challenging me to improve. I'd especially like to thank Dr. Lang and her lab for assistance with sampling, improving sampling protocols, and lab analyses. I want to thank my lab partners for their support and assistance with sampling, Halley Carruthers, Kristen Laccetti, Kristiaan Merritt, and especially Dr. Eilea Knotts, who offered statistical and writing advice throughout the writing process. They have all truly been a treasure to work with and have enriched my life during my time as a student.

Next, I'd like to thank all of the wonderful people who have helped me with sampling and lab analyses during the past few years. First, the team at Charleston Scuba, especially Tom Robinson, Ed Chapman, and Brad Nelson, who cheerfully and carefully collected our samples. Secondly, those who helped with sampling before and during cruises, especially Jacob Vincent, Malayika Vincent, Jessica Frankle, and Bryan Benitez-

Nelson. They and the Charleston Scuba team made even the most nausea-inducing sampling days enjoyable. Finally, the many people who processed lab samples, including John Williams and Krystyn Kibler for helping with HPLC, Jaquan High for the sediment grain analyses, and Dr. Angela Knapp and her lab for the nutrient analyses.

Lastly, I would also like to thank my funding sources, the International Women's Fishing Association, Conservation Education Foundation of the South Carolina Wildlife Federation, the South Carolina American Water Works Association, the Southeastern Estuarine Research Society, the School of the Earth, Ocean and Environment, and NSF Grant #OCE 1736557 for providing financial support during my research.

ABSTRACT

Benthic microalgae (BMA) play essential roles in food webs and regulating nutrient exchange at the sediment-water interface in continental shelf ecosystems. However, shelf BMA are not widely studied due to the difficulties sampling the upper few millimeters of shelf sediments. A few published studies have highlighted the high spatiotemporal distribution of BMA, but detailed explanations for this known variability are limited. The objectives of this study were to quantify BMA biomass variability on scales of cm to km and relate these measurements to *in situ* nutrient concentrations, sediment grain size, *in situ* irradiance, depth, and other environmental factors. Water and sediment samples for BMA and porewater nutrient analyses were collected by SCUBA divers on 11 nearshore cruises in 2018-2020 off Charleston, SC. BMA accounted for over half of total microalgal chlorophyll *a*, with BMA biomass reaching as high as 10 times that of phytoplankton in the overlying waters. High variability in BMA biomass was observed between and within sites, indicating BMA are likely influenced by small-scale (<1 m) environmental differences. BMA biomass was positively correlated with percentage of fine grain sediments, but not with dissolved inorganic nitrogen (DIN) concentrations in either the water column, porewater, or submarine groundwater. However, porewater DIN was much higher than in the water column, suggesting that higher BMA biomass may be more dependent on N from the sediments rather than the overlying waters. Understanding how BMA vary spatially can be useful for making

larger generalizations about BMA distribution over continental shelves and for modeling BMA biomass, production, and contribution to both benthic and pelagic food webs.

TABLE OF CONTENTS

ACKNOWLEDGEMENTS	iii
ABSTRACT.....	v
LIST OF FIGURES	viii
CHAPTER 1: INTRODUCTION	1
CHAPTER 2: METHODS	4
CHAPTER 3: RESULTS	9
CHAPTER 4: DISCUSSION.....	26
REFERENCES	34

LIST OF FIGURES

Figure 2.1: Map of sampling locations near Charleston, SC	8
Figure 3.1: Temperature ($^{\circ}\text{C}$), salinity, and pH for cruises	17
Figure 3.2: Percent sediment grain size (μm)	18
Figure 3.3: Mean phytoplankton chlorophyll <i>a</i> ($\mu\text{g l}^{-1}$)	18
Figure 3.4: Water column accessory pigment concentrations ($\mu\text{g l}^{-1}$)	19
Figure 3.5: Ratio of (a) water column chlorophyll <i>b</i> to chlorophyll <i>a</i>	20
Figure 3.6: BMA chlorophyll <i>a</i> (mg m^{-2}) on sampling dates	20
Figure 3.7: Benthic photopigments on sampling dates	21
Figure 3.8: Mean benthic chlorophyll <i>a</i> (mg m^{-2}) to depth	22
Figure 3.9: Water column nutrient concentrations (μM)	23
Figure 3.10: Submarine groundwater well nutrient concentrations (μM)	24
Figure 3.11: Porewater ammonium (NH_4) concentrations (μM)	25
Figure 4.1: Curves of required sample size	33

CHAPTER 1

INTRODUCTION

Benthic microalgae (BMA) play a critical role in continental shelf ecology and benthic biogeochemistry. As a substantial contributor to total primary productivity (Cahoon & Cooke 1992; Jahnke et al., 2000; Cesbron et al., 2019) and total chlorophyll *a* (chl *a*) in the surface sediments of continental shelves (Cahoon & Cooke 1992; Nelson et al. 1999; Jahnke et al. 2000; Grippo et al. 2010), BMA are significant sources of organic carbon for both benthic and pelagic consumers (Kang et al. 2003; Mallin et al. 2005; Chouvelon et al. 2015). Additionally, BMA influence nutrient and oxygen exchange at the sediment-water interface (Jahnke et al. 2000; Reay et al. 1995; Sundbäck et al. 1991; Sundbäck et al. 2004). Despite BMA importance in shallow shelf sediments, detailed studies of shelf BMA have been hindered by difficulties collecting sediment samples with the undisturbed microlayer that contains the bulk of photosynthetically active BMA. Phytoplankton chl *a* measurements are more easily collected, and relative changes in surface chl *a* can be obtained through satellites that measure ocean-color. By contrast, sediment chl *a* requires more labor-intensive sampling, and productivity measurements to this point are mostly made through *in situ* benthic chambers. While several studies have shown the importance and contribution of BMA to shelf microalgal biomass, most are

limited by adequate replication, large spatiotemporal scales, and precise sampling of the upper few mm of intact sediment surface microlayers.

In the South Atlantic Bight (SAB) continental shelf region, which extends from Cape Hatteras, NC, to West Palm Beach, FL, BMA biomass often exceeds that of integrated phytoplankton on an areal basis, with BMA accounting for up to 80% of total chl *a* and benthic primary production over 84% of the shelf area (Cahoon & Cooke 1992; Jahnke et al. 2000; Nelson et al. 1999). As a sandy, sedimentary shelf, the SAB is representative of an estimated 70% of global continental margins (Emery 1968), making conclusions drawn from studies of this shelf comparable to other temperate, sandy shelves worldwide.

Sediments are a very heterogeneous environment, with widely varied conditions only millimeters apart (Anderson & Meadows 1978; Marinelli et al. 1998; Pischedda et al. 2008). Given this, it is likely that BMA exhibit as much variance within a site, in a scale of only several cm, as between sites, on a scale as large as several km. Previous studies have shown that BMA biomass is highly variable over space and time with a high level of spatial patchiness (Cahoon et al. 1990; Sandulli & Pinckney 1990; Cahoon & Cooke 1992; Cahoon & Laws 1993; Nelson et al. 1999). However, few have adequately quantified this variation and attempted to relate the variation to environmental variables. Quantifying BMA spatial variation may provide insights into the factors that influence BMA growth and biomass. Furthermore, a determination of the adequate number of samples to reliably assess spatial variation is necessary to reliably compare BMA measurements across space and time (MacIntyre et al. 1996).

The objective of this study was to assess BMA biomass (as chl *a*) and community composition on the South Carolina inner continental shelf and correlate BMA biomass with factors (e.g., sediment composition, nutrient concentration, *in situ* irradiance) that may influence biomass on large (km) to small (cm) spatial scales. My primary hypotheses were that benthic chl *a* would be greater than the integrated water column chl *a* on an areal basis, and that the variability in BMA biomass was greater on km scales (between sampling sites) than cm scales (sampling within a site).

CHAPTER 2

METHODS

2.1 FIELD SAMPLING

Sampling was conducted along the SC continental shelf offshore Charleston (Fig. 2.1). Samples were collected from 11 locations during nine cruises between June 2018 and March 2020 (Table 2.1). The March 2020 cruise was completed just prior to the COVID-19 pandemic, so only hydrological conditions, pigment data, and porewater nutrient concentrations are available for that date. Cruise dates were chosen to capture seasonal variability, with at least one cruise in the autumn, spring, and summer months each year. Sampling locations were selected primarily from the inner continental shelf (depth <20 m), with two sampling locations in the midshelf region (20-40 m). Four sites (stations 7, 9, 11, and 12) contained wells for sampling submarine groundwater. Bottom water, well water, and sediment samples were collected by SCUBA divers to preserve sample integrity and minimize disturbance.

Irradiance (photosynthetically available radiation (PAR)), water temperature, and depth were recorded at 1 m intervals from surface to bottom at each site. Irradiance was measured using a 4 π LI-250A light meter. Water temperature, pH, salinity, chl *a* fluorescence, dissolved O₂, and depth were measured using a 650 MDS YSI with 6820 Multiparameter Sonde at 1 m intervals throughout the water column. For sites that were deeper than 15 m, water was collected from the bottom using a horizontal Niskin bottle and measured immediately on deck in a bucket.

Surface water for nutrient analyses were collected by filtering water through pre-combusted (500°C for 5 h) Advantec GF/75 flat filters (0.3 µm pore size, P/N GF7547MM) into acid-washed HDPE bottles. Divers pumped bottom and well water into acid-washed Kynar bags using a Guzzler. Water was then filtered through an Acropak 0.2 µm filter (P/N 12039) and collected in acid-washed HDPE bottles. Samples were kept on dry ice and then stored at -20°C until analysis.

Paired water samples for phytoplankton chl *a* were collected at each station: a surface sample from the top 1 m of water and a bottom sample from ca. 0.5 m above the sediments. Surface samples were collected using an integrated vertical sampler (PVC bailer) for the upper 1 m, and bottom samples were collected with a horizontal Niskin sampler that was lowered to 0.5 m above the sediment. Water samples were stored on ice in a darkened cooler, filtered within 24-48 h on Sterlitech glass fiber filters (0.7 µm pore size, P/N F2500), and stored at -80°C.

Divers used small, clear butyrate core tubes (1 cm² x 6 cm) to randomly collect 10 sediment samples over a 1m² area for benthic chl *a* at each site. Core tubes were capped and stored on ice in a darkened cooler. The upper 1 cm of sediment was sectioned from each core tube within 48 h and stored at -80°C. Large acrylic plastic core tubes (85 cm² x 30 cm) were used to collect sediments for porewater extraction. Cores were capped immediately after collection and stored on ice in a darkened cooler. Care was taken to ensure that core tubes were tightly sealed and transported vertically to minimize porewater mixing during and after collection. Within 8 h of collection, porewater samples were obtained at 2-5 cm intervals, depending on sediment porosity, starting at a depth of 2-3 cm below the sediment surface. Rhizon SMS samplers (Number 19.21.01F, 0.15 µm

pore size, 2.5 mm diameter) were inserted horizontally through pre-drilled holes in the core tube to extract the pore water. The collection points were separated by 2-5 cm vertically in the sediment to prevent oversampling (Seeberg-Elverfeldt et al. 2005). The amount of water extracted varied based on sediment porosity, but the target volume for extraction was 2 ml. Porewater was frozen in 2 ml acid-washed microfuge tubes on dry ice and stored at -80°C.

2.2 LAB ANALYSES

Filters and sediments were analyzed using high performance liquid chromatography (HPLC) to identify and quantify photopigments (Pinckney et al. 2001). Samples were lyophilized for 24 h at -50° C, placed in 90% acetone (1.00 ml), sonicated, and extracted at -20° C for 18-20 h. Filtered extracts (250 µl) were injected into a Shimadzu HPLC with a monomeric column (Rainin Microsorb-MV, 0.46 cm × 10 cm, 3 µm) and a polymeric (Vydac 201TP54, 0.46 cm × 25 cm, 5 µm) reverse-phase C18 column in series. A nonlinear binary gradient consisting of the solvents 80% methanol:20% 0.50 M ammonium acetate and 80% methanol:20% acetone was used for pigment separations (Pinckney et al. 1996). Absorption spectra and chromatograms (440 ± 4 nm) were acquired using a Shimadzu SPD-M10v photodiode array detector. Pigment peaks were identified by comparison of retention times and absorption spectra with pure standards (DHI, Denmark). The synthetic carotenoid β-apo-8'-carotenal (Sigma) was used as an internal standard.

After acetone extraction, the sediments were dried, weighed, and sorted by sediment grain size. Grain size and distribution were measured using a CamsizerTM (Retsch). The instrument used digital image analysis with a dual camera system that

measured and recorded particle size distribution, shape, and additional parameters as they fell through a feeder slot.

Ammonium (NH_4^+) concentrations were measured using the fluorescent OPA method (Holmes et al. 1999) and Trilogy Turner Fluorometer with a Turner Ammonium Snap-In Module (7200-067). The chemiluminescent method outlined by Braman & Hendrix (1989) was used to measure water column nitrate and nitrite ($\text{NO}_3^- + \text{NO}_2^-$). Total dissolved nitrogen (TDN) concentrations were calculated using persulfate oxidation of TDN to NO_3^- (Knapp et al. 2005), and nitrate, nitrite, and ammonium concentrations were subtracted from TDN to calculate dissolved organic nitrogen (DON) concentrations.

2.3 STATISTICAL ANALYSES

The data were analyzed with the statistical program R, v. 3.6.0. In general, the data were not normally distributed with heterogeneous variances. The non-parametric Wilcoxon signed-ranks test was used to determine whether the surface and bottom phytoplankton biomass samples were different on dates when both were collected, and whether the variation within a site differed from variation between sites on a sampling date. The non-parametric Kruskal-Wallis one-way analysis of variance was used to assess whether BMA and phytoplankton biomass differed between sampling dates and between stations, and the Dunn post-hoc test with Bonferroni correction was used when the results were significant. Spearman's correlation analysis was used for testing whether benthic chl *a* was correlated to the following variables: grain size, percent fine sediments, temperature, PAR diffuse attenuation coefficient, salinity, pH, and water depth.

Table 2.1: Station names, latitude and longitude (digital degrees, N and W), number of times sampled, and average depth (m) of sampling sites.

Station	Latitude	Longitude	Sampled	Average Depth
7	32.7069	79.6611	8	10.3
9	32.7564	79.6632	2	10.6
11	32.7671	79.6414	4	10.9
12	32.7266	79.6151	8	10.3
14	32.7479	79.5692	6	12.6
15	32.7878	79.5947	4	11.7
SNZ02	32.6767	79.5537	1	11.7
SNZ03	32.7093	79.5196	2	12.5
SNZ04	32.7422	79.4791	1	11.9
SNZ06	32.5862	79.2729	1	32.0
SNZ07	32.6448	79.2124	1	32.0

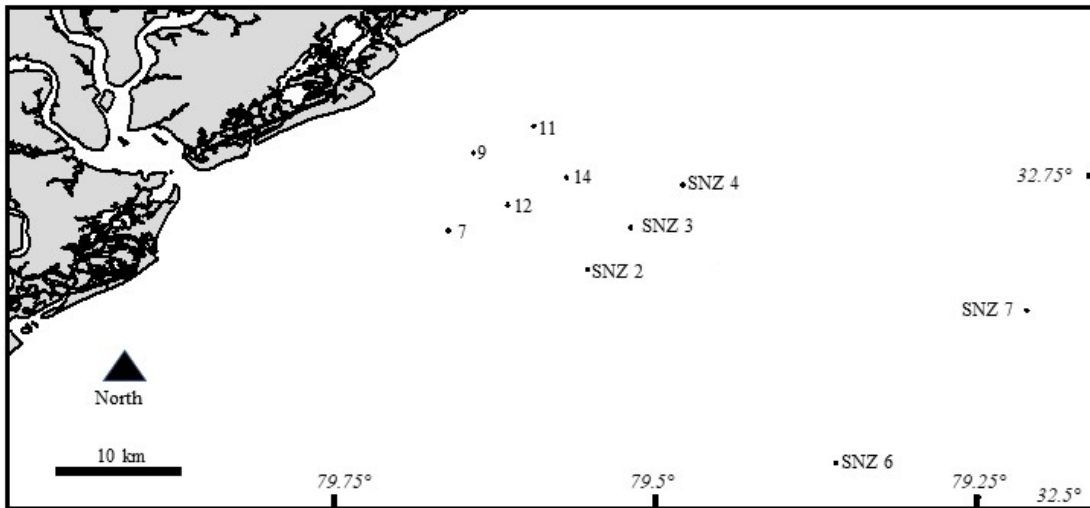


Figure 2.1: Map of sampling locations near Charleston, SC.

CHAPTER 3

RESULTS

3.1 HYDROGRAPHICAL CONDITIONS

Eleven sites were sampled over 9 cruises from June 2018 to March 2020. The two most frequently sampled stations were stations 7 ($n = 8$) and 12 ($n = 8$). Stations SNZ02, SNZ04, SNZ06, and SNZ07 were each only sampled once. All stations were on the inner shelf, with depths between 7 and 14 m, except for stations SNZ06 and SNZ07, which were each 32 m deep and located on the midshelf.

Sea surface salinities were 33.9 ± 1.9 (mean \pm 1 sd) with an observed range of 28.3 to 36.4 (Fig. 3.1). Salinity stratification was observed in October 2018, suggesting there was a freshwater lens over the surface following riverine freshwater discharge from Hurricane Florence in September 2018. Surface pH was 8.02 ± 0.15 with a range of 7.59 to 8.32. pH fell mostly between 7.9 and 8.1, except for the autumn months in 2018 and March 2020, which exceeded 8.1. Sea surface temperatures were $23.7 \pm 4.4^\circ \text{C}$ with a range of 13.9°C in March 2020 to 28.9°C in August 2019. Thermal stratification was observed during the late spring and summer cruise dates. However, for most dates, surface and bottom temperature differed less than 3°C . Both temperature and salinity exerted influence on benthic biomass. BMA chl *a* was strongly correlated with average water column temperature ($p < 0.001$; $R = 0.71$) and correlated with average water column salinity ($p = 0.0014$; $R = 0.51$). BMA biomass was also weakly correlated with water column surface pH ($p = 0.0412$; $R = -0.34$).

Diffuse attenuation coefficients (k_d for PAR) for all sites were $0.40 \pm 0.37 \text{ m}^{-1}$ with a range of 0.15 to 1.67 m^{-1} (Table 3.1). During the October and November 2018 cruises, turbidity was high with k_d values >1.00 and poor visibility observed by divers. With the exception of the autumn 2018 and March 2020 cruises, however, the bottom sediments received $>1\%$ surface irradiance. BMA chl *a* did not correlate with k_d ($p = 0.8362$; $R = -0.037$) or water depth ($p = 0.256$; $R = 0.19$).

3.2 SEDIMENT GRAIN ANALYSES

The mean sediment grain size for all samples was $510 \pm 301 \text{ }\mu\text{m}$ (mean $\pm 1 \text{ sd}$) with a range of 249 to $1493 \text{ }\mu\text{m}$. Sediments at the sampling stations were primarily sandy, with over 80% of sediments between 125 and $1000 \text{ }\mu\text{m}$. Two exceptions were stations SNZ03 and 9, which contained more shell hash and a higher percentage of larger sediments. Mean grain size for station SNZ03 was $858 \text{ }\mu\text{m}$, and 29% of sediments were greater than $1000 \text{ }\mu\text{m}$. Mean grain size for station 9 was $1356 \text{ }\mu\text{m}$, with 54% of sediments were greater than $1000 \text{ }\mu\text{m}$. Sediment grain sizes were not determined for stations SNZ06 and SNZ07. Mean sediment grain size did not correlate with mean BMA chl *a* ($p = 0.259$; $R = -0.23$) or station depth ($p = 0.446$; $R = 0.16$). Chl *a* was also not correlated with the percentage of very fine sediment ($< 125 \text{ }\mu\text{m}$) ($p = 0.067$, $R = 0.36$), but had a weak positive correlation with very fine and small sediments ($<250 \text{ }\mu\text{m}$) ($p = 0.026$, $R = 0.44$) (Fig. 3.2).

3.3 PHYTOPLANKTON BIOMASS AND PIGMENT COMPOSITION

A total of 38 surface samples and 27 bottom samples were collected for phytoplankton analyses. Mean water column chl *a* for all sampling dates was $1.57 \pm 1.62 \text{ }\mu\text{g l}^{-1}$ with a range of 0.37 to $2.99 \text{ }\mu\text{g l}^{-1}$ (Fig. 3.3). Surface chl *a* was $1.51 \pm 1.63 \text{ }\mu\text{g l}^{-1}$

with a range of 0.36 to 7.99 $\mu\text{g l}^{-1}$, and bottom chl *a* was $1.18 \pm 0.65 \mu\text{g l}^{-1}$ with a range of 0.38 to 2.38 $\mu\text{g l}^{-1}$. Surface biomass was highest in October and November 2018, four to eight times higher than for other sampling dates. Mean surface chl *a* excluding October and November 2018 values was $1.00 \pm 0.43 \mu\text{g l}^{-1}$ and ranged from 0.36 to 2.44 $\mu\text{g l}^{-1}$.

The median phytoplankton chl *a* did not differ between surface and bottom for paired phytoplankton samples (Wilcoxon ranked sum test; $n = 26$; $p = 0.1388$). Median surface phytoplankton biomass was not different for any of the dates except the two cruises in October 2018 ($7.04 \pm 1.34 \mu\text{g l}^{-1}$) and November 2018 ($4.68 \pm 0.75 \mu\text{g l}^{-1}$) ($p = 0.0229$).

Fucoxanthin, an accessory pigment indicative of diatoms, was the most abundant planktonic pigment for all cruises except August 2018 (Fig. 3.4). Fucoxanthin concentration for the water column ranged from 0.21 to 2.78 $\mu\text{g l}^{-1}$ and accounted for $16.8 \pm 3.5\%$ total carotenoids. The next most abundant pigment, zeaxanthin (cyanobacteria), was $6.0 \pm 5.4\%$ total pigment, ranging from 0.04 to 0.41 $\mu\text{g l}^{-1}$. August 2018 was the only date when the zeaxanthin:fucoxanthin ratio exceeded 1 (Fig. 3.5a). Chl *b* (green algae) was very low in summer months ($<0.05 \mu\text{g l}^{-1}$) and was highest in March 2020. Chl *b* concentrations relative to chl *a* were greatest in the spring months of both years (Fig. 3.5b). The highest ratio (0.23 chl *b*:chl *a*) was in March 2020, followed by April 2019 (0.11 chl *b*:chl *a*). Alloxanthin (cryptophytes) and peridinin (dinoflagellates) were also observed in the water column, although in low concentrations ($\leq 5\%$ of total pigment).

3.4 BMA BIOMASS AND PIGMENT COMPOSITION

BMA chl *a* for the top 10 mm of sediment was $41.36 \pm 20.68 \text{ mg m}^{-2}$ with a range of 7.48 to 93.96 mg m^{-2} (Table 3.1). Chl *a* concentrations were strongly influenced by both location ($p < 0.001$) and sampling date ($p < 0.001$). BMA biomass was highest during the August sampling dates for both years (Fig. 3.6). Chl *a* for August 2018 was $76.09 \pm 26.90 \text{ mg m}^{-2}$ ($n = 3$), and chl *a* for August 2019 was $66.60 \pm 19.09 \text{ mg m}^{-2}$ ($n = 6$). The lowest observed values were in March 2020 at $19.83 \pm 9.15 \text{ mg m}^{-2}$. For all other cruises, mean chl *a* fell between 25 and 45 mg m^{-2} .

The diatom pigment fucoxanthin was the most abundantly observed accessory pigment and accounted for over 80% ($81.3 \pm 8.3\%$) total carotenoids (Fig. 3.7). Fucoxanthin was $1.41 \pm 0.85 \text{ ug g}^{-1}$ dry sediment with a range of 0.27 to 3.37 ug g^{-1} . Fucoxanthin concentrations showed similar temporal patterns to chl *a* and were highest in August 2018 and 2019. The cyanobacterial pigment zeaxanthin accounted for less than 2% of total carotenoids; however, zeaxanthin was present at every site and sampling date. The ratio of zeaxanthin:fucoxanthin was low, with a mean of <0.05 , indicating that cyanobacteria were only present in small amounts. The green algal pigment chl *b* was present for every date except October and November 2018, and the chl *b*:chl *a* ratio was highest in the spring months. Peridinin was found in low concentrations ($< 0.01 \text{ ug g}^{-1}$ dry sediment) in April and May 2019.

3.5 COMPARISON OF BENTHIC SEDIMENT AND WATER COLUMN BIOMASS AND PIGMENTS

On an area basis, benthic chl *a* exceeded water column chl *a* for 29 of the 36 dates and stations sampled (Fig. 3.9). The seven samples where the benthic:water column

biomass ratio was <1 were collected from shallow sites located less than 11 km from shore: stations 7, 11, 12, and 14. Four of those samples were collected during October and November 2018, when water column chl *a* was significantly higher than other sampling dates, indicating that a phytoplankton bloom altered the benthic:water column ratio to <1 , rather than a decrease in BMA biomass. Two sites in March 2020 experienced a ratio of <1 . While the water column chl *a* was not different from other dates, benthic chl *a* was the lowest sampled during the entire study.

For both the water column and benthic sediment, the most abundant photosynthetic pigment was fucoxanthin, indicating that diatoms were the most dominant primary producers in the South Carolina shelf. Zeaxanthin (cyanobacteria) was present in both the water column and the sediments for every site and dates sampled; however, the water column had higher concentrations, even exceeding fucoxanthin concentrations in August 2018, while only trace ($<0.10 \mu\text{g g}^{-1}$ sed) amounts of the pigment were found in the sediments. Alloxanthin (cryptophytes) was present in the water column in high concentrations during autumn 2018, and in trace amounts for several other months, but it was only found in the sediments in August 2019. Pigments that were present in both the water column and the sediments include diadinoxanthin, peridinin (dinoflagellates), prasinoxanthin, and chl *b* (green algae).

3.6 VARIATION OF BMA BIOMASS

Small-scale (cm) variability of BMA chl *a* was calculated using the coefficient of variation (CV) for replicates ($n = 10$) collected at the same site in a $<1 \text{ m}^2$ area. For large scale variability (km), the CV was measured using all the pooled samples collected during a sampling date ($n = 20-60$). A non-parametric Wilcoxon signed-ranks test was

used to pair each site-specific CV with the pooled CV for that cruise date and determine if there was a difference between small-scale CV and large-scale CV. Variation between stations (km) was greater than variation within a site (cm) ($p < 0.001$), suggesting that although BMA experience patchiness and small-scale variation, large scale changes in environmental conditions correspond with about twice the variation as small-scale changes in the sediment microenvironment.

Variation within a site (cm) was greatest during the late summer and lowest during the late autumn. The CV for all sampling dates was $22 \pm 11\%$, and reached its highest value at station 12 in August 2018 at 52%. Variation ranged from 18% to 30%, with the exception of November 2018, where the CV for both sites sampled was $<10\%$. Large scale variation (km) (CV for multiple sites on a single date) was $40 \pm 19\%$ and ranged from 20 to 76%, roughly twice that as within a site. This suggests that although large scale environmental changes more strongly influence changes BMA biomass, small microscale environmental conditions also influence patterns in BMA distribution.

3.7 NUTRIENT ANALYSES

For overlying waters, total dissolved nitrogen (TDN) was $7.69 \pm 3.21 \mu\text{M}$, of which a significant portion ($7.27 \pm 2.52 \mu\text{M}$) was dissolved organic nitrogen (DON) (Fig. 3.9). Water column dissolved inorganic nutrients (DIN) concentrations were very low, with almost two-thirds of all NH_4 , NO_3 , and NO_2 measurements below detection limits ($<25 \text{ nM}$), and NO_3 and NO_2 exceeding $1 \mu\text{M}$ on only one sampling date (November 2018). DIN concentrations were highest during October and November 2018 and March 2020. Ammonium (NH_4) concentrations in the water column were low ($0.10 \pm 0.15 \mu\text{M}$). Bottom water NH_4 was higher than surface water NH_4 in April and early May 2019. For

most cruise dates, $<1 \mu\text{M}$ of NH_4 was present in the water column. October and November 2018 were the two exceptions to these patterns, as the surface waters contained higher concentrations of DON and DIN. Of the 6 submarine groundwater samples collected from wells, NH_4 exceeded water column NH_4 by several orders of magnitude (Fig. 3.10). The mean well water TDN concentration was $45.77 \pm 18.65 \mu\text{M}$. Mean well water NH_4 was $17.11 \pm 22.07 \mu\text{M}$, with a range of 0.17 to $54.95 \mu\text{M}$.

2-3 porewater cores were sampled at each station, and nutrient concentration variation within the cores was high within sites, even when sampled at the same sediment depth (Fig. 3.11). The mean porewater NH_4 concentration was $38.54 \pm 36.91 \mu\text{M}$ for the upper 2-18 cm of sediments, exceeding water column NH_4 every time both were sampled. There was no discernable pattern for NH_4 vertical distribution within a core. For most cores, NH_4 concentration increased with sediment depth. However, many also showed a decrease in concentration with depth or appeared unchanged. Porewater NH_4 was not correlated with depth in sediment (Spearman's correlation analysis, $p = 0.087$, $R = 0.17$).

Surface phytoplankton chl *a* concentrations were correlated with surface water NH_4 concentrations (Spearman's correlation analysis, $p = 0.01844$, $R = 0.477$). Neither bottom phytoplankton chl *a* nor BMA chl *a* were correlated with DIN concentrations in submarine groundwater, porewater, or the water column ($p > 0.05$).

Table 3.1: Summary of water column and benthic chl *a* measurements for June 2018 to March 2020. k_d = irradiance diffuse attenuation coefficient for PAR (m^{-1}); water column chl *a* = integrated water column chl *a* ($mg\ m^{-2}$); BMA chl *a* = mean BMA chl *a* for top 1 cm ($mg\ m^{-2}$); sediment:water column chl *a* = ratio of mean BMA chl *a* to integrated phytoplankton chl *a*.

Date	Station	Depth (m)	k_d (m^{-1})	Water column chl <i>a</i> ($mg\ m^{-2}$)	BMA chl <i>a</i> ($mg\ m^{-2}$)	Sediment: water column chl <i>a</i>
7-Jun-18	7	7.3	0.23	5.74	48.28 ± 10.54	8.42
7-Jun-18	12	11.8	0.26	12.69	7.48 ± 1.90	0.59
7-Aug-18	7	7.3	-	9.19	-	-
7-Aug-18	11	10	-	9.90	-	-
7-Aug-18	12	9.6	0.33	11.43	73.58 ± 38.40	6.43
7-Aug-18	14	12.7	0.28	12.55	60.47 ± 13.01	4.82
7-Aug-18	15	12.1	0.30	9.93	93.96 ± 11.80	9.46
15-Oct-18	7	11.1	1.23	88.70	31.17 ± 10.35	0.35
15-Oct-18	12	10.1	1.08	61.53	21.50 ± 1.94	0.35
19-Nov-18	11	11.5	1.26	59.88	48.81 ± 4.04	0.82
19-Nov-18	12	9.6	1.67	39.86	21.82 ± 2.18	0.55
29-Apr-19	7	10.9	0.28	9.25	31.29 ± 7.21	3.38
29-Apr-19	9	11.6	-	5.96	22.77 ± 9.21	3.82
29-Apr-19	11	10.9	0.21	9.14	47.75 ± 8.26	5.22
29-Apr-19	12	9.8	0.22	5.15	25.30 ± 3.71	4.91
29-Apr-19	14	10.8	0.23	6.80	35.21 ± 10.16	5.18
29-Apr-19	15	11.3	0.24	9.74	38.03 ± 12.44	3.90
6-May-19	7	11.5	0.19	10.57	33.77 ± 4.94	3.19
6-May-19	9	9.7	0.28	16.78	20.80 ± 8.31	1.24
6-May-19	14	12.6	-	13.12	35.07 ± 3.15	2.67
6-May-19	15	11.1	0.26	17.80	41.72 ± 3.52	2.34
23-May-19	SNZ02	11.7	0.21	10.18	37.24 ± 6.90	3.66
23-May-19	SNZ03	11.9	0.19	10.86	44.93 ± 20.06	4.14
23-May-19	SNZ04	11.9	0.17	15.76	43.20 ± 7.33	2.74
24-May-19	7	11.5	0.28	22.55	50.28 ± 10.87	2.23
24-May-19	12	10.3	0.19	17.97	29.46 ± 5.10	1.64
24-May-19	14	12.9	0.19	10.71	47.80 ± 8.42	4.46
5-Aug-19	11	11.3	0.23	11.01	78.86 ± 10.02	7.16
5-Aug-19	14	13.0	0.27	16.15	59.96 ± 12.09	3.71

Date	Site	Depth (m)	k_d (m^{-1})	Water column chl a ($mg\ m^{-2}$)	BMA chl a ($mg\ m^{-2}$)	Sediment: water column chl a
5-Aug-19	15	12.1	0.28	23.32	55.76 ± 8.14	2.39
6-Aug-19	SNZ03	13.2	0.25	7.74	79.48 ± 32.57	10.27
6-Aug-19	7	12.2	0.32	18.36	69.56 ± 17.62	3.79
6-Aug-19	12	10.3	0.28	9.93	56.28 ± 6.37	5.67
10-Mar-20	SNZ06	32	0.15	11.84	18.17 ± 6.83	1.53
10-Mar-20	SNZ07	32	0.16	12.48	32.82 ± 10.17	2.63
11-Mar-20	7	11.0	0.59	21.79	15.63 ± 1.54	0.72
11-Mar-20	12	10.8	0.46	7.00	16.28 ± 2.90	2.33
11-Mar-20	14	13.7	0.89	18.87	14.41 ± 1.69	0.76

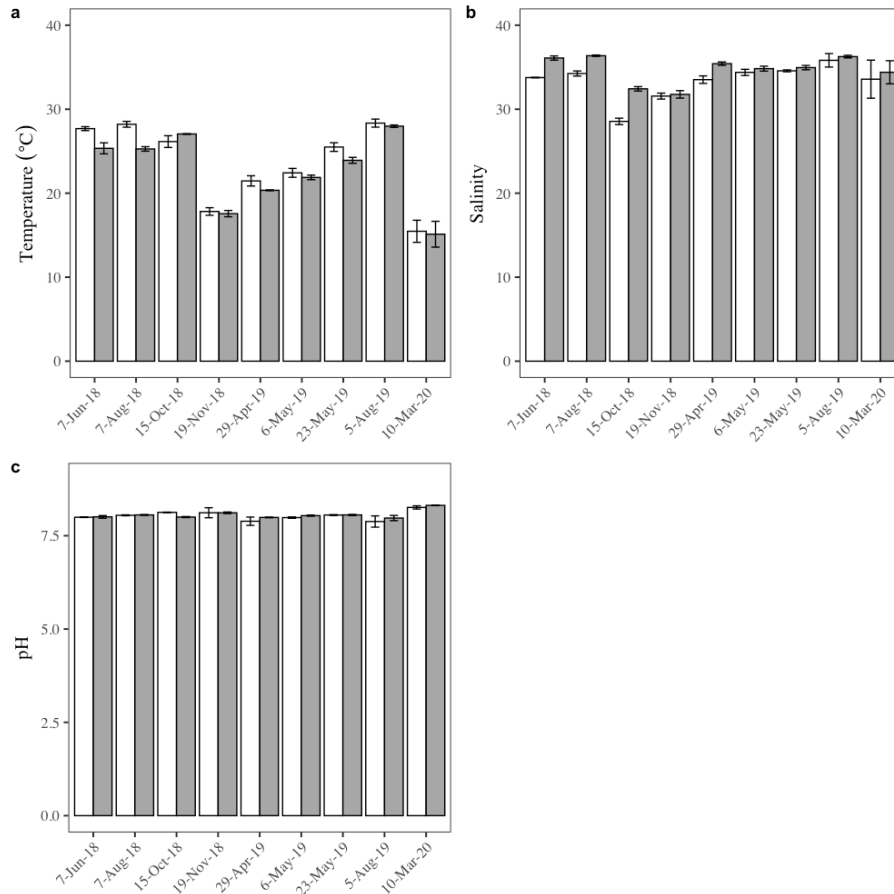


Figure 3.1: (a) Temperature ($^{\circ}C$), (b) salinity, and (c) pH for cruises. White bars are surface water values, and grey bars are bottom water values. Error bars are ± 1 standard deviation.

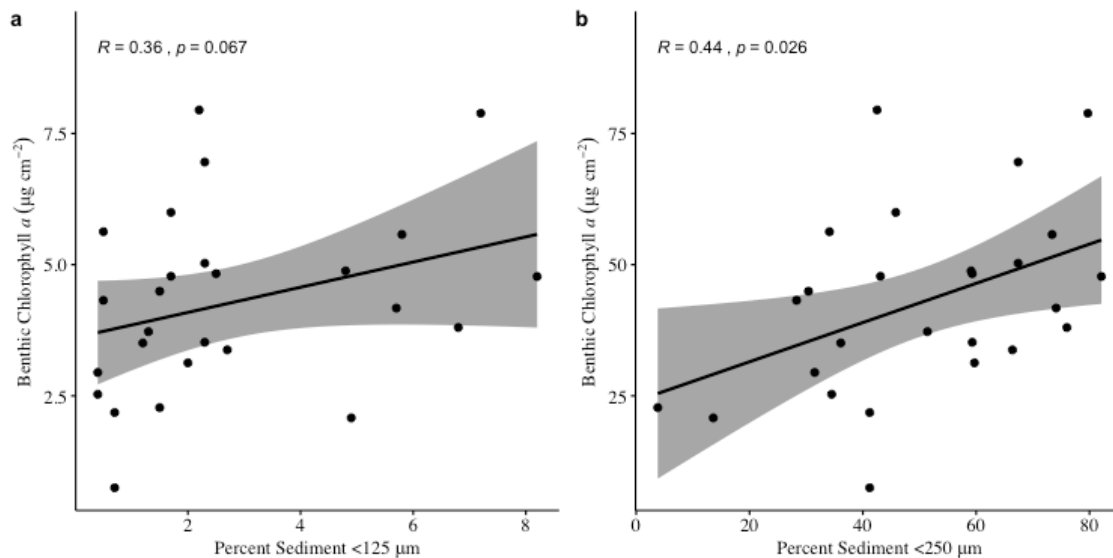


Figure 3.2: Percent sediment grain size (μm) and benthic chlorophyll a (mg m^{-2}). Grey bar is 95% confidence interval.

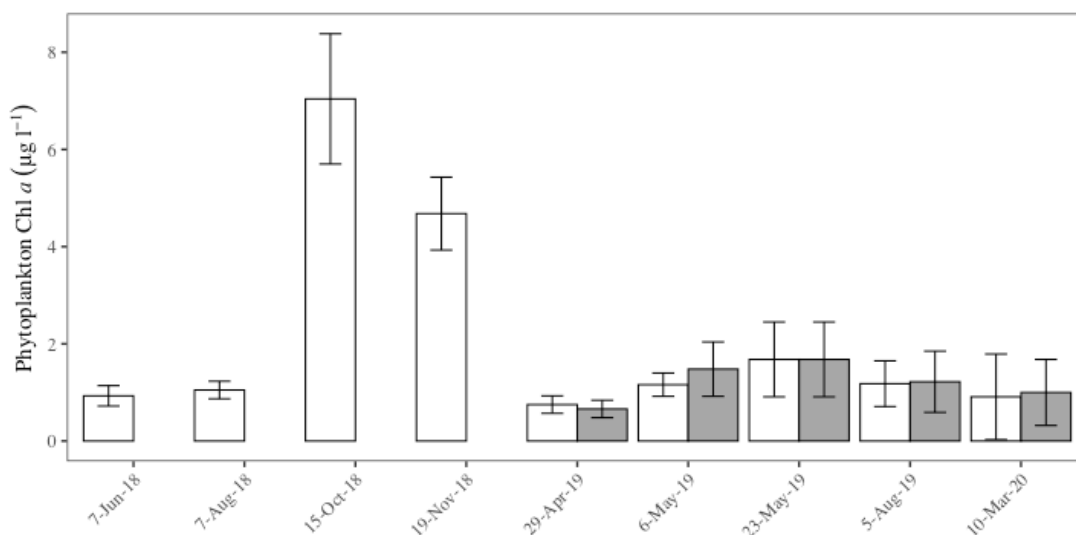


Figure 3.3: Mean phytoplankton chlorophyll a ($\mu\text{g l}^{-1}$) on sampling dates. White bars indicate samples collected at the surface, and grey indicates samples collected directly above the bottom. No bottom samples were collected prior to April 2019. Error bars are \pm 1 standard deviation.

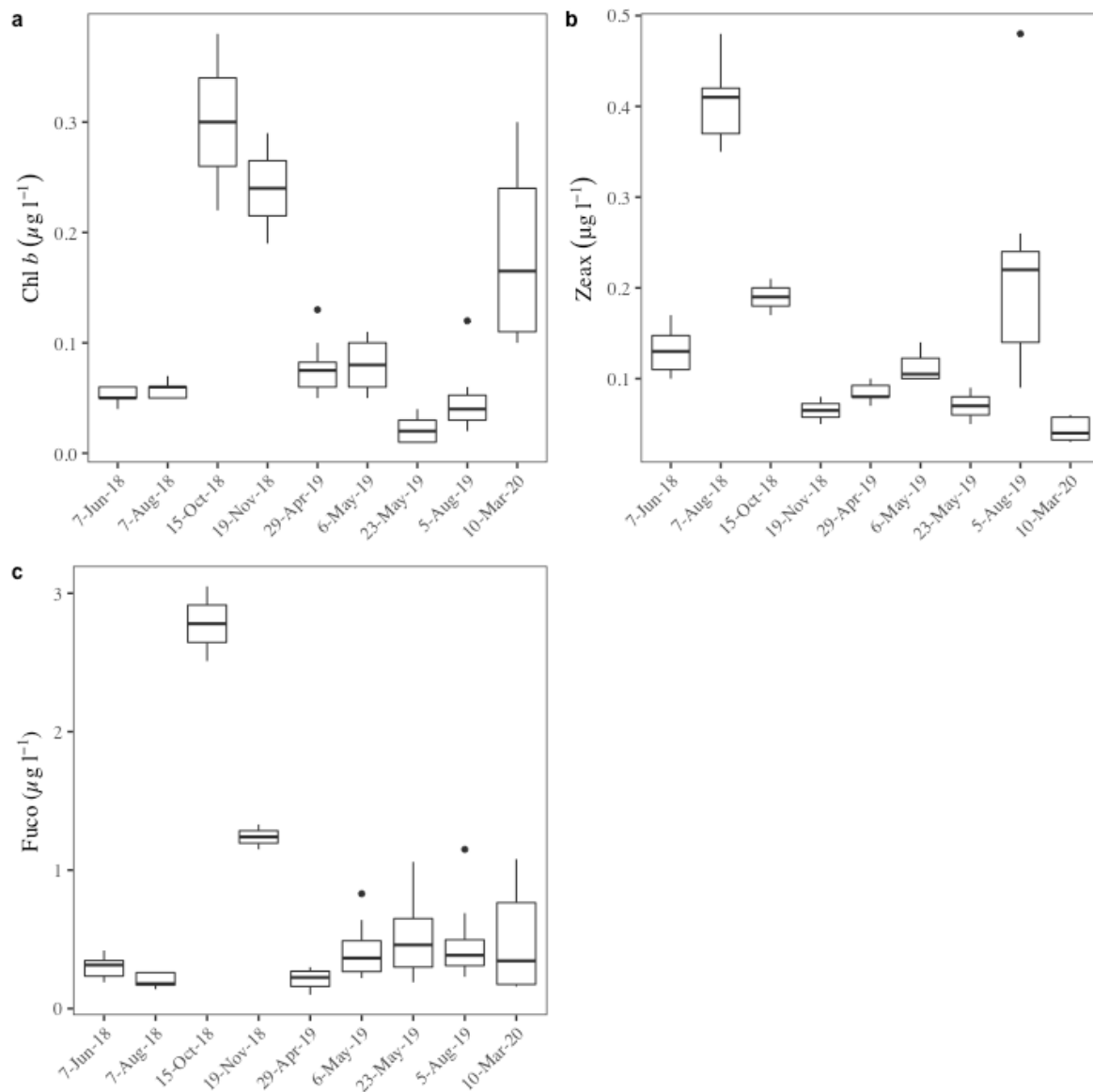


Figure 3.4: Water column accessory pigment concentrations ($\mu\text{g l}^{-1}$) for all sampling dates and sites. (a) Chl *b* = Chlorophyll *b*; (b) Zeax = Zeaxanthin; (c) Fuco = Fucoxanthin. Samples prior to April 2019 contain only surface water samples, and samples from April 2019 and later are averaged with surface and bottom samples.

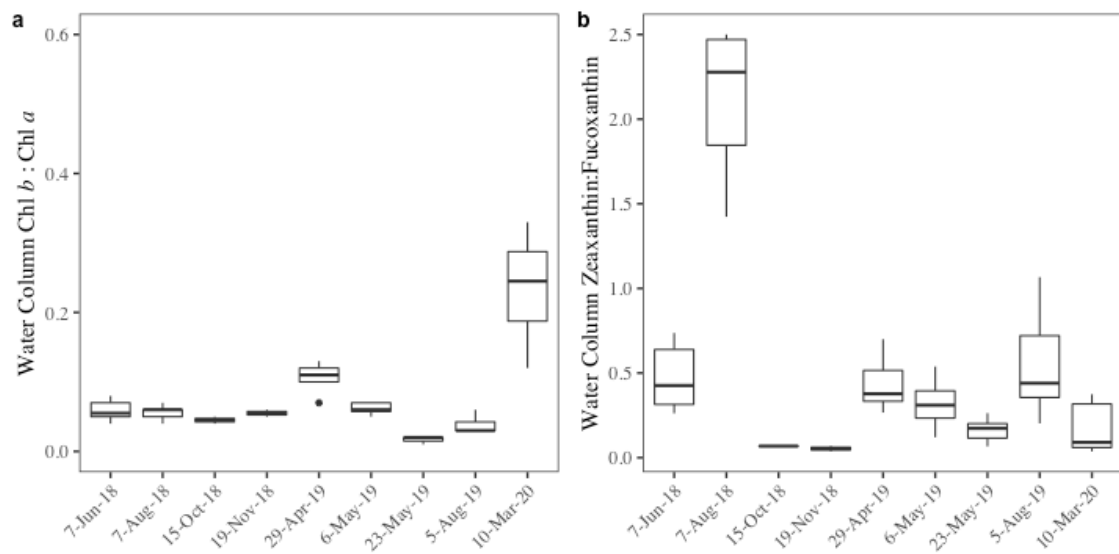


Figure 3.5: Ratio of (a) water column chlorophyll *b* to chlorophyll *a* and (b) water column zeaxanthin to fucoxanthin. Samples prior to April 2019 contain only surface water samples, and samples from April 2019 and later are averaged with surface and bottom samples.

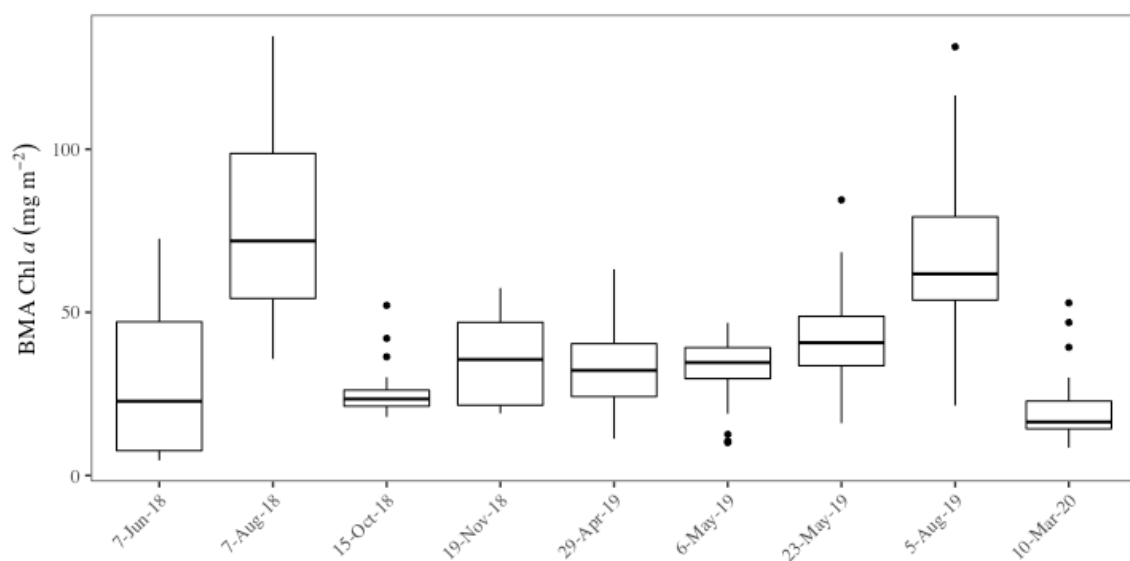


Figure 3.6: BMA chlorophyll *a* (mg m⁻²) on sampling dates. BMA chl *a* is pooled between all sites sampled on cruise date.

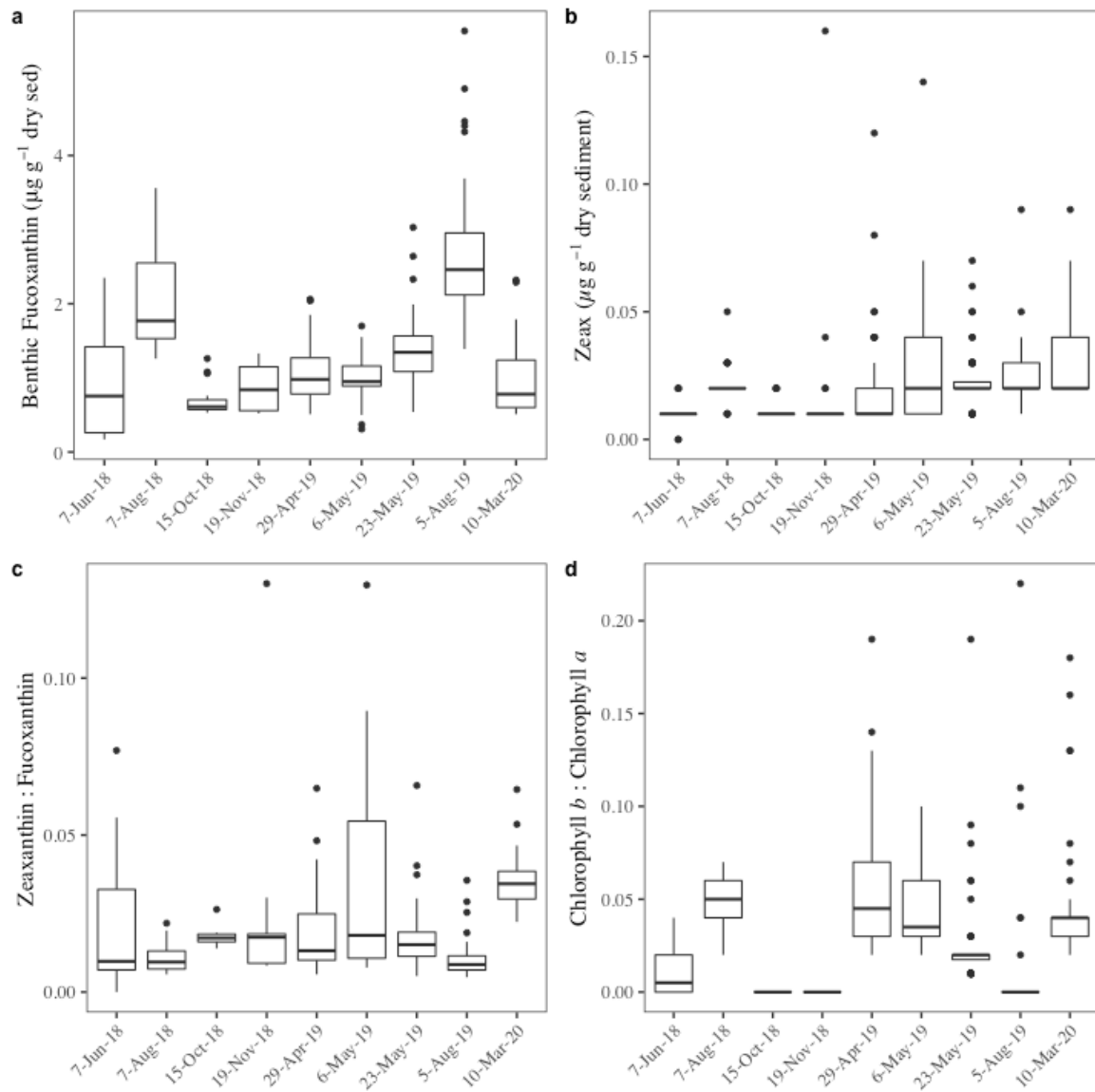


Figure 3.7: Benthic photopigments on sampling dates. (a) Benthic fucoxanthin ($\mu\text{g g}^{-1}$ dry sediment); (b) benthic zeaxanthin ($\mu\text{g g}^{-1}$ dry sediment); (c) ratio of zeaxanthin:fucoxanthin; (d) ratio of chlorophyll *b*:chlorophyll *a*.

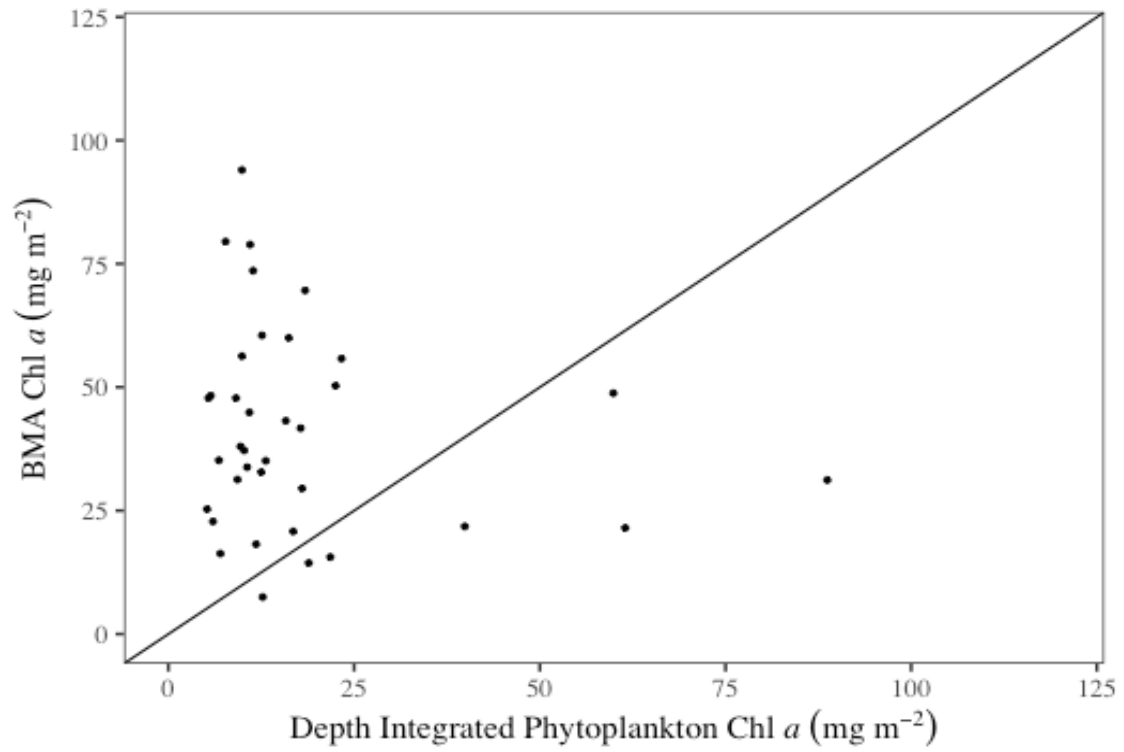


Figure 3.8: Mean benthic chlorophyll *a* (mg m⁻²) to depth integrated phytoplankton chlorophyll *a* (mg m⁻²). Diagonal line represents an equal benthic:water column biomass ratio.

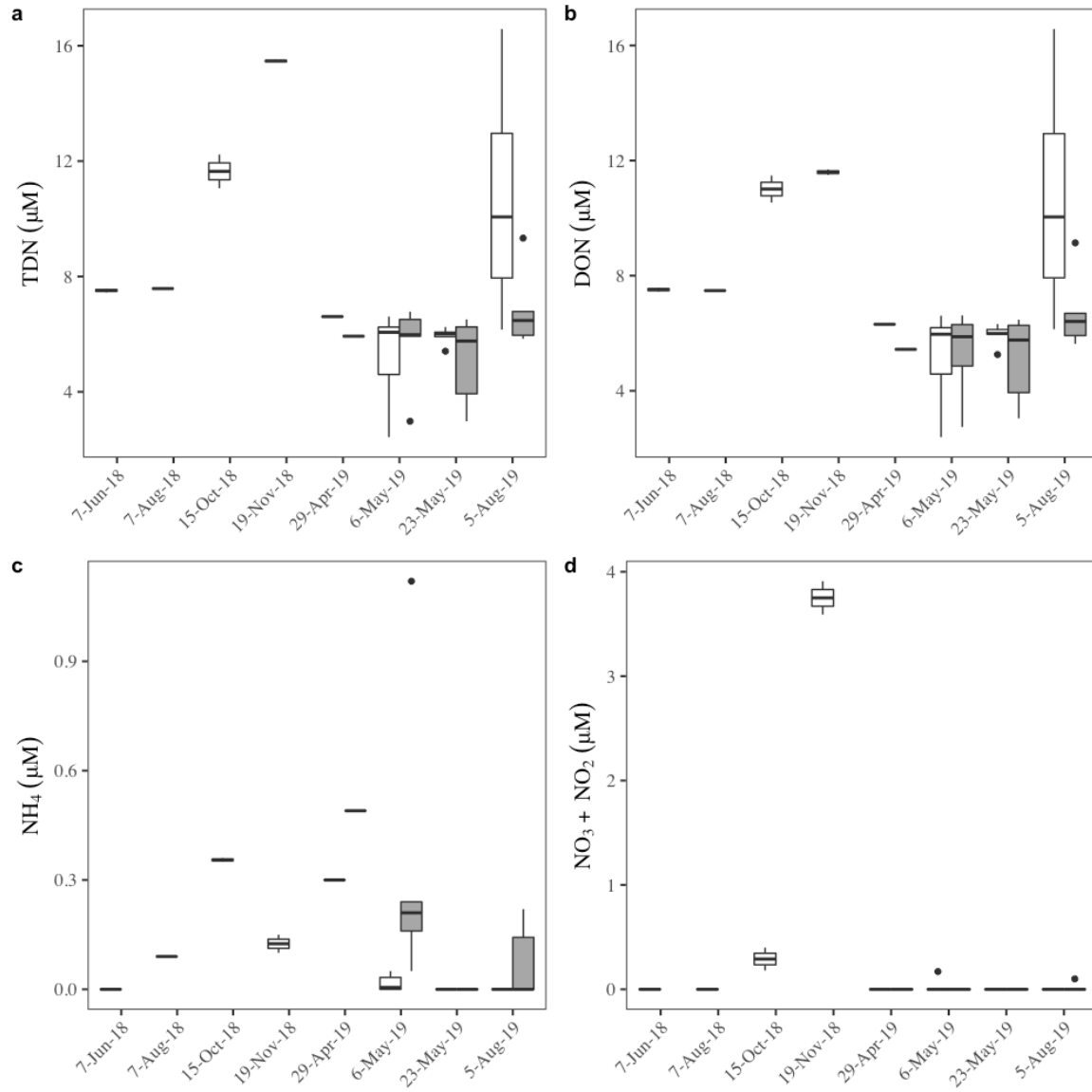


Figure 3.9: Water column nutrient concentrations (μM) for (a) total dissolved nitrogen (TDN), (b) dissolved organic nitrogen (DON), (c) ammonium (NH₄), and (d) nitrate (NO₃) and nitrite (NO₂). White bars indicate samples collected at the surface, and grey indicates samples collected directly above the bottom. No bottom samples were collected prior to April 2019.

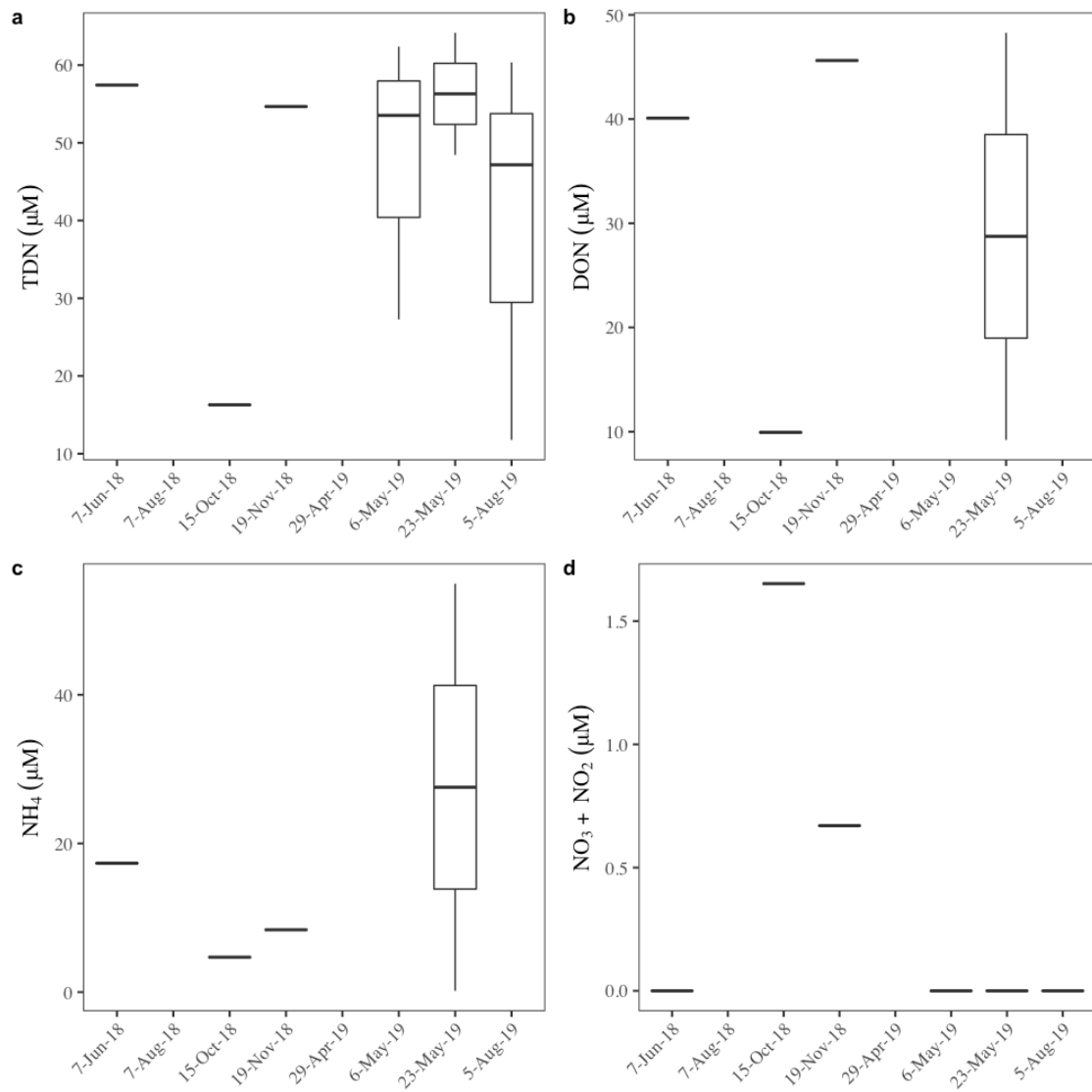


Figure 3.10: Submarine groundwater well nutrient concentrations (μM) for (a) total dissolved nitrogen (TDN), (b) dissolved organic nitrogen (DON), (c) ammonium (NH₄), and (d) nitrate (NO₃) and nitrite (NO₂).

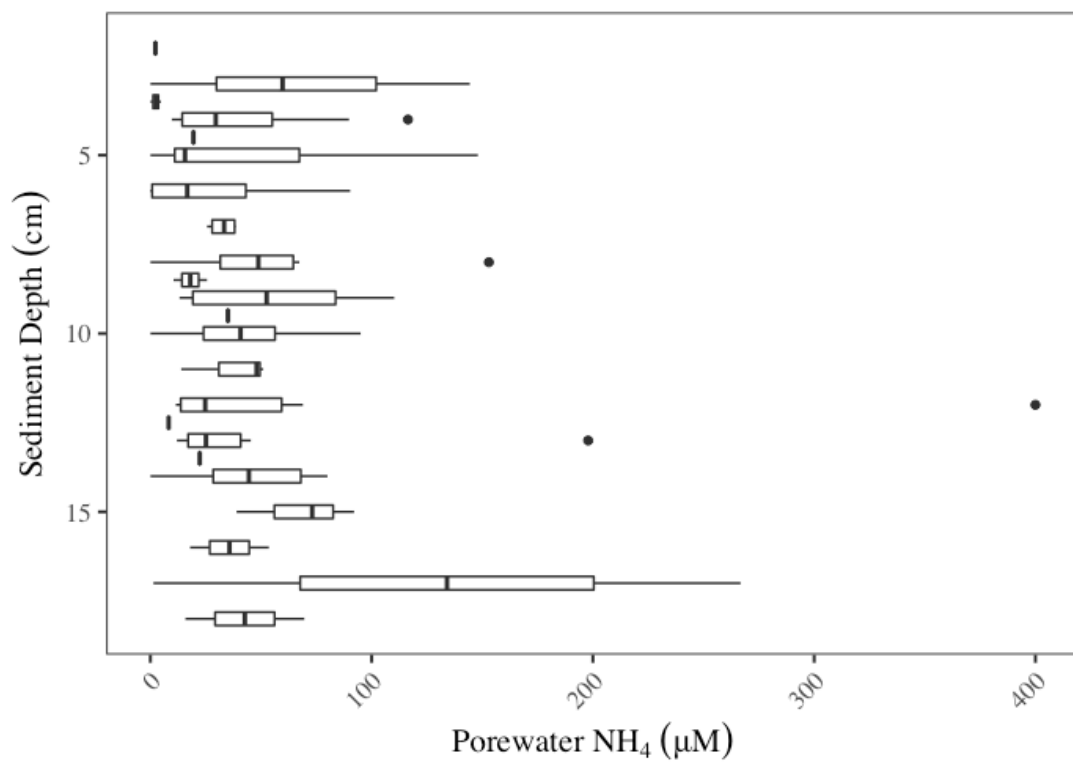


Figure 3.11: Porewater ammonium (NH_4) concentrations (μM) at depths sampled.

CHAPTER 4

DISCUSSION

4.1 BMA AND PHYTOPLANKTON BIOMASS

Our results demonstrate that BMA constitute an average 70% of the photosynthetic biomass of the SAB inner continental shelf. Benthic sediment chl *a* was greater than water column chl *a* for almost every site and date, reaching as much as ten times that of the integrated phytoplankton biomass. BMA biomass was consistent with values reported by previous studies in the SAB, which also found that benthic biomass in the SAB often exceeded that of the water column (Cahoon & Cooke 1992; Nelson et al. 1999; Jahnke et al. 2000). The high concentration of microalgal biomass in the sediments cannot be ignored when drawing conclusions for continental shelf contribution to regional and global cycling, and weighing contribution of water column phytoplankton more heavily when modeling shelf biomass and production can lead to serious underestimations.

Several mechanisms have been proposed to explain why water column chl *a* is generally lower than benthic chl *a*. N limitation has been exhibited in the SAB water column and sediments (Rao et al. 2008; Sedwick et al. 2018). Given the low ammonium and nitrate concentrations observed by this study and others in the SAB (Bishop et al. 1980; Verity et al. 1993; Marinelli et al. 1998; Rao et al. 2007), it is likely that for most of our study, the water column exhibited N limitation that promoted low phytoplankton biomass. By contrast, our study found that both porewater and submarine groundwater

NH₄ concentrations usually exceeded water column ammonium by several orders of magnitude, suggesting that BMA are not totally dependent on water column N but rather have access to sediment-derived N, whether from high rates of N remineralization (Marinelli et al. 1998; Jahnke et al. 2005) or submarine groundwater discharge (Pinckney 2018), which allows a larger accumulation of BMA biomass. Our study did not find a correlation between any nutrient concentrations and BMA biomass; however, this is likely because we measured static nutrient concentrations rather than nutrient fluxes.

During October and November 2018, water column chl *a* exceeded benthic chl *a* by up to 2.5 times. This was likely a result of excessive nutrient loading in the water column and a consequential phytoplankton bloom. Hurricane Florence passed through SC in September 2018, setting a new state rainfall record and peak flood stage records in several rivers in South Carolina (Stewart & Berg 2019). During sampling in October and November 2018, high turbidity, which is typically observed after hurricanes (Nelson et al. 1999), and higher DON and DIN concentrations suggested that flood waters were still draining through Charleston at that time, leading to the phytoplankton blooms. A low benthic:water column chl *a* ratio was also found at two sites in March 2020; however, this was likely caused by lower BMA biomass, rather than elevated phytoplankton biomass in the water column. Lower light availability may have been the cause, since these two sites experienced the highest k_d values apart from the autumn 2018 cruise dates. Although our study did not show a relationship between k_d and BMA biomass, irradiance has been previously shown to influence biomass and productivity (Cahoon & Cooke 1992; Jahnke et al. 2000).

Diatoms were the most dominant algal group in both the water column and the sediments. Zeaxanthin concentrations exceeded fucoxanthin in August 2018 in the water column, but that was not repeated in August 2019, although the zeaxanthin:fucoxanthin ratio was higher during August 2019 than any other month in 2019. This suggests that there may be some seasonality in cyanobacteria in the water column, although it is unclear whether August 2019 experienced a lower bloom of cyanobacteria or August 2018 experienced a higher bloom. Chl *b*:chl *a* was also anomalously high in the water column during March 2020, indicating that more chlorophytes may have been present during that time. Diatoms were the most prevalent group in the sediments with little variation in community composition. Diatoms, cyanobacteria, chlorophytes, and cryptophytes which have all been noted as present in the SAB water column and sediments, with diatoms making up the majority of both communities (Cahoon and Laws 1993; Nelson et al. 1999; Jahnke et al. 2000; McGee et al. 2008).

Although this study did not measure photosynthetic rates, Jahnke et al. (2000) showed that BMA are significant primary producers in the SAB, with average BMA primary productivity almost equal to water column productivity. Benthic chambers, the primary source of benthic productivity measurements in the SAB, have been noted for their inaccuracy in permeable sediments by altering porewater flow (Archer & Devol 1992; Huettel et al. 2014). Because of this, measuring changes in BMA biomass using sediment cores may be a sufficient alternate for studying the relative contribution of BMA to carbon and nutrient cycling in the SAB.

4.2 VARIATION IN BMA BIOMASS

Shelf benthic microalgae have been shown to be heterogeneously distributed with a highly variable biomass on small and large scales (Cahoon & Cooke 1992; Nelson et al. 1999). Considering the challenges for sampling shelf sediments, understanding variables that influence benthic biomass would help to understand how changes in microenvironments affect BMA. Productivity models also require taking into account variation in BMA distribution (Bartoli et al. 2003; Serôdio et al. 2001), as inaccurate measurements of BMA spatial coverage may lead to over or underestimations of benthic productivity. BMA distribution may not only be a product of external variables, such as grazing (Sommer 1999; Hillebrand 2008), but may also exert influence on its environment as well. For example, variability in BMA distribution has been shown to at least partially affect higher trophic levels by influencing meiofauna distribution (Blanchard 1990) as well as nutrient fluxes (Bartoli et al. 2003).

Because of the number of replicate cores ($n = 10$) collected at each station, we were able to observe patterns of variability on small scales and compare them to large scale variation. We found that variation between sites on a sampling date was around twice the variation within a site, indicating that changes over large scales affect BMA biomass more strongly than smaller scale changes. There was still some variability between replicates at each site, mostly between 20-30%, suggesting that BMA exhibit spatial patchiness. Some sites likely experienced a more uniform distribution, with <10% variance between replicates. Low variation was more common on dates when biomass was low.

Our data showed a similar pattern to Nelson et al. (1999), who found that variability between replicate cores explained less than 1% of total variability, with <20% coefficient of variation for the means of replicate cores. Given this, it is reasonable to suggest that variance of biomass within a site explains only a small amount of total variability for our sites as well. However, since some of our sites experienced variation of up to 60%, small scale environmental fluctuations should not be discounted as they likely exert a varying amount of influence on BMA biomass.

BMA spatial patchiness should be considered when sampling to ensure that sampling is representative of the true population. BMA often exhibit a clumped distribution, and patch size can vary from <4 cm² to almost 200 cm² (Blanchard 1990; Sanulli & Pinckney 1999). Collecting too few replicates may introduce error if all replicates occur only in patches with high microalgal biomass or in areas between patches with low biomass. In order to estimate the number of replicates required for sampling within the relative accuracy of the mean, we used the variance found within each sample site and the t-value from a normal distribution with a significance of 0.05 (Eckblad 1991). Our current sampling procedure of 10 replicates per site averaged between ±15-20% of the true mean of the population (Fig. 4.1). Many BMA studies likely use too few replicates, as using only 2-3 replicates for our sites yielded an estimated accuracy of ±35-40% of the true mean of the population. Therefore, more samples should be collected when possible to account for variation in patch size and space between patches.

4.3 PREDICTORS OF BMA BIOMASS

Our study found that temperature, surface pH, and salinity were predictors of benthic biomass, but depth and light availability were not. The correlation between

salinity and biomass was not strong, and temperature was likely a function of temporal changes, which were also shown to influence biomass. Despite other studies having shown that benthic biomass decreases with increasing depth and decreasing light (Cahoon 1999; Nelson et al. 1999), neither were strong predictors of biomass in our study. This is likely because our stations were mostly of a similar depth (7-14 m) and they consistently received over 1% surface PAR. However, BMA have also been found in the SAB midshelf (Cahoon & Cooke 1992; Cahoon & Laws 1993; Nelson et al. 1999) and continental slope (McGee et al. 2008), so while light availability may affect biomass and species of BMA, the SAB sediments still receive adequate light for BMA growth.

Sediment type and grain size have often been suggested as predictors for benthic biomass; however, results are inconsistent, showing a positive, negative, or even no relationship between grain size and BMA biomass (Billerbeck et al. 2007; Cahoon et al. 1999; Cahoon et al. 2012; First & Hallibaugh 2010; Jesus et al. 2009). Our study showed only a weak correlation between small and fine sediments and BMA biomass, and no correlation between BMA biomass and mean sediment grain size. Other studies have shown relationships between grain size and biomass (Cahoon et al. 1999; Cahoon et al. 2012; First and Hallibaugh 2010), however these studies were conducted in salt marshes and shallow coastal habitats, not along the continental shelf. It seems that along the South Carolina shelf, the percentage of fine sediments and grain size may be predictors in biomass variability.

Variables that were not measured or interactions between multiple variables may also be responsible for variance in BMA biomass. Organic matter, sediment compaction, redox gradient, and porewater pH have all been suggested as possible controls on

biomass variability (Cahoon et al. 1999; Cahoon et al. 2012; First and Hallibaugh 2010). Bioturbation and grazing have also been hypothesized to influence BMA patchiness and small scale variability (Nelson et al. 1999). Bioturbation affects spatial distribution of porewater nutrients, which was heterogeneously distributed within our sites (Marinelli et al. 1998), and microenvironmental conditions (Aller 1980; Pischedda et al. 2008). Benthic grazers may also control BMA biomass and distribution, as BMA offer concentrated food source for benthic grazers and deposit feeders. Several possible BMA grazers have been noted as present in the SAB, such as demersal zooplankton, small polychaetes, and meiofauna (Cahoon & Tronzo 1992; Nelson et al. 1999).

Our study was limited in breadth of sampling locations and depths, with the two most visited sites in the same ~12 m isobath. Only two stations exceeded 15 m depth, and these were each sampled once. While the large number of samples and varied sampling dates give a comprehensive look of BMA biomass along the South Carolina inner shelf, further research should be done at greater depths. Studies in the midshelf and outer shelf are necessary to understand BMA dynamics on the shelf. A better understanding of spatiotemporal variability in benthic BMA biomass is necessary for improving knowledge of benthic shelf trophodynamics as well as nutrient dynamics along the sediment-water interface.

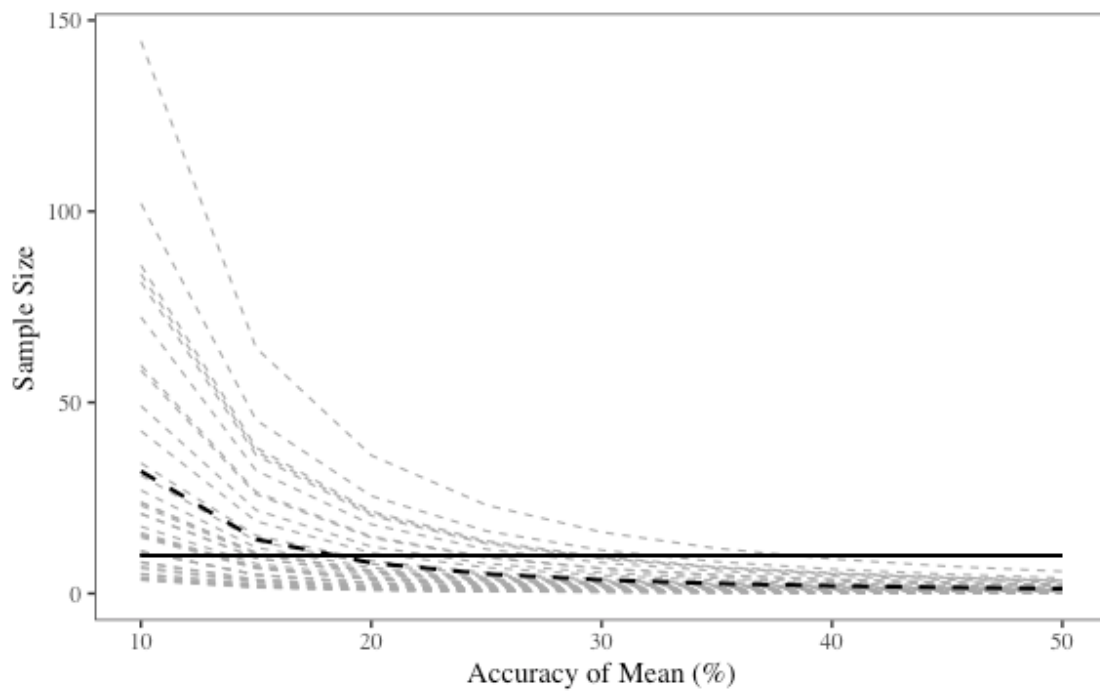


Figure 4.1: Curves of required sample size and accuracy from the mean from samples. Light grey dotted lines are from individual cruises. Black dotted line is average of all cruises. Black horizontal line represents sample size used during this study ($n = 10$).

REFERENCES

- Archer, D., & Devol, A. (1992). Benthic oxygen fluxes on the Washington shelf and slope: A comparison of in situ microelectrode and chamber flux measurements. *Limnology and Oceanography*, 37(3), 614-629.
- Aller, R. C. (1980). Quantifying solute distributions in the bioturbated zone of marine sediments by defining an average microenvironment. *Geochimica et Cosmochimica Acta*, 44(12), 1955-1965.
- Anderson, J. G., & Meadows, P. S. (1978). Microenvironments in marine sediments. *Proceedings of the Royal Society of Edinburgh, Section B: Biological Sciences*, 76(1-3), 1-16.
- Bartoli, M., Nizzoli, D., & Viaroli, P. (2003). Microphytobenthos activity and fluxes at the sediment-water interface: interactions and spatial variability. *Aquatic Ecology*, 37(4), 341-349.
- Billerbeck, M., Røy, H., Bosselmann, K., & Huettel, M. (2007). Benthic photosynthesis in submerged Wadden Sea intertidal flats. *Estuarine, Coastal and Shelf Science*, 71(3-4), 704-716.
- Bishop, S.S., Yoder, J.A., & Paffenhofer, G.A. (1980). Phytoplankton and nutrient variability along a cross-shelf transect off Savannah, Georgia, USA. *Estuarine and Coastal Marine Science*, 11(4), 359-368.
- Blanchard, G. (1990). Overlapping microscale dispersion patterns of meiofauna and microphytobenthos. *Marine Ecology Progress Series*, 68(1-2), 101-111.
- Braman, R.S., & Hendrix, S.A. (1989). Nanogram nitrite and nitrate determination in environmental and biological materials by vanadium (III) reduction with chemiluminescence detection. *Analytical chemistry*, 61(24), 2715-2718.
- Cahoon, L.B., Redman, R.S., & Tronzo, C.R. (1990). Benthic microalgal biomass in sediments in Onslow Bay, North Carolina. *Estuarine, Coastal and Shelf Science*, 31(6), 805-816.
- Cahoon, L.B., & Cooke, J.E. (1992). Benthic microalgal production in Onslow Bay, North Carolina, USA. *Marine Ecology Progress Series*, 84, 185-196.

- Cahoon, L.B., & Tronzo, C.R. (1992). Quantitative estimates of demersal zooplankton abundance in Onslow Bay, North Carolina, USA. *Marine Ecology Progress Series*, 197-200.
- Cahoon, L. B., & Laws, R. A. (1993). Benthic diatoms from the North Carolina continental shelf: inner and mid shelf 1. *Journal of Phycology*, 29(3), 257-263.
- Cahoon, L.B. (1999). The role of benthic microalgae in neritic ecosystems. *Oceanography and Marine Biology Annual Review*, 37, 47–86.
- Cahoon, L.B., Nearhoof, J.E., & Tilton, C.L. (1999). Sediment grain size effect on benthic microalgal biomass in shallow aquatic ecosystems. *Estuaries*, 22(3B), 735-741.
- Cahoon, L.B., Carey, E.S., & Blum, J.E. (2012). Benthic microalgal biomass on ocean beaches: effects of sediment grain size and beach renourishment. *Journal of Coastal Research*, 28(4), 853–859.
- Cesbron, F., Murrell, M.C., Hagy, M.E., Jeffrey, W.H., Patterson III, W.F., & Caffrey, J.M. (2019). Patterns in phytoplankton and benthic production on the shallow continental shelf in the northeastern Gulf of Mexico. *Continental Shelf Research*, 179, 105-114.
- Chouvelon, T., Schaal, G., Grall, J., Pernet, F., Perdriau, M., A-Pernet, E.J., & Le Bris, H. (2015). Isotope and fatty acid trends along continental shelf depth gradients: Inshore versus offshore hydrological influences on benthic trophic functioning. *Progress in Oceanography*, 138, 158-175.
- Eckblad, J.W. (1991). How many samples should be taken? *BioScience*, 41(5), 346-348.
- Emery, K.O. (1968). Relict sediments on continental shelves of the world: *American Association of Petroleum Geologists Bulletin*, v. 52.
- First, M. R., & Hollibaugh, J. T. (2010). Environmental factors shaping microbial community structure in salt marsh sediments. *Marine Ecology Progress Series*, 399, 15-26.
- Grippo, M.A., Fleeger, J.W., Rabalais, N.N., Condrey, R., & Carman, K.R. (2010). Contribution of phytoplankton and benthic microalgae to inner shelf sediments of the north-central Gulf of Mexico. *Continental Shelf Research*, 30(5), 456-466.
- Hillebrand, H. (2008). Grazing regulates the spatial variability of periphyton biomass. *Ecology*, 89(1), 165-173.
- Huettel, M., Berg, P., & Kostka, J. E. (2014). Benthic exchange and biogeochemical cycling in permeable sediments. *Annual Reviews in Marine Science*, 6, 23–51.

- Holmes, R. M., Aminot, A., K  rouel, R., Hooker, B. A., & Peterson, B. J. (1999). A simple and precise method for measuring ammonium in marine and freshwater ecosystems. *Canadian Journal of Fisheries and Aquatic Sciences*, 56(10), 1801-1808.
- Jahnke, R.A., Nelson, J.R., Marinelli, R.L., & Eckman, J.E. (2000). Benthic flux of biogenic elements on the Southeastern US continental shelf: influence of pore water advective transport and benthic microalgae. *Continental Shelf Research*, 20, 109-127.
- Jahnke, R., Richards, M., Nelson, J., Roberston, C., Rao, A., & Jahnke, D. (2005). Organic matter remineralization and pore water exchange rate in permeable South Atlantic Bight continental shelf sediments. *Continental Shelf Research*, 25(12-13), 1433-1452.
- Kang, C.K., Kim, J.B., Lee, K.S., Kim, J.B., Lee, P.Y., & Hong, J.S. (2003). Trophic importance of benthic microalgae to macrozoobenthos in coastal bay systems in Korea: dual stable C and N isotope analyses. *Marine Ecology Progress Series*, 259, 79-92.
- Knapp, A.N., Sigman, D.M., & Lipschultz, F. (2005). N isotopic composition of dissolved organic nitrogen and nitrate at the Bermuda Atlantic Time-series Study site. *Global Biogeochemical Cycles*, 19(1).
- MacIntyre, H.L., Geider, R.J., & Miller, D.C. (1996). Microphytobenthos: the ecological role of the "secret garden" of unvegetated, shallow-water marine habitats. I. Distribution, abundance and primary production. *Estuaries*, 19(2), 186-201.
- Mallin, M.A., Cahoon, L.B., & Durako, M.J. (2005). Contrasting food-web support bases for adjoining river-influenced and non-river influenced continental shelf ecosystems. *Estuarine, Coastal and Shelf Science*, 62(1-2), 55-62.
- Marinelli, R.L., Jahnke, R.A., Craven, D.B., Nelson, J.R., & Eckman, J.E. (1998). Sediment nutrient dynamics on the South Atlantic Bight continental shelf. *Limnological Oceanography*, 43(6), 1305-1320.
- McGee, D., Laws, R.A., & Cahoon, L.B. (2008). Live benthic diatoms from the upper continental slope: extending the limits of marine primary production. *Marine Ecology Progress Series*, 356, 103-112.
- Nelson, J.R., Eckman, J.E., Roberston, C.Y., Marinelli, R.L., & Jahnke, R.A. (1999). Benthic microalgal biomass and irradiance at the sea floor on the continental shelf of the South Atlantic Bight: spatial and temporal variability and storm effects. *Continental Shelf Research*, 19, 477-505.

- Pinckney, J.L., Millie, D.F., Howe, K.E., Paerl, H.W., & Hurley, J.P. (1996). Flow scintillation counting of ^{14}C -labeled microalgal photosynthetic pigments. *Journal of Plankton Research*, 18(10), 1867-1880.
- Pinckney, J.L., Richardson, T.L., Millie, D. F., & Paerl, H. W. (2001). Application of photopigment biomarkers for quantifying microalgal community composition and in situ growth rates. *Organic Geochemistry*, 32(4), 585-595.
- Pinckney, J. L. (2018). A Mini-Review of the Contribution of Benthic Microalgae to the Ecology of the Continental Shelf in the South Atlantic Bight. *Estuaries and Coasts*, 41(7), 2070-2078.
- Pischedda, L., Poggiale, J.C., Cuny, P., & Gilbert, F. (2008). Imaging oxygen distribution in marine sediments. The importance of bioturbation and sediment heterogeneity. *Acta biotheoretica*, 56(1-2), 123-135.
- Rao, A.M.F., McCarthy, M.J., Gardner, W.S., & Jahnke, R.A. (2007). Respiration and denitrification in permeable continental shelf deposits on the South Atlantic Bight: rates of carbon and nitrogen cycling from sediment column experiments. *Continental Shelf Research*, 27, 1801-1819.
- Rao, A. M., McCarthy, M. J., Gardner, W. S., & Jahnke, R. A. (2008). Respiration and denitrification in permeable continental shelf deposits on the South Atlantic Bight: N_2 : Ar and isotope pairing measurements in sediment column experiments. *Continental Shelf Research*, 28(4-5), 602-613.
- Reay, W.G., Gallagher, D.L., & Simmons Jr, G.M. (1995). Sediment-water column oxygen and nutrient fluxes in nearshore environments of the lower Delmarva Peninsula, USA. *Marine Ecology Progress Series*, 215-227.
- Sandulli, R., & Pinckney, J. (1999). Patch sizes and spatial patterns of meiobenthic copepods and benthic microalgae in sandy sediments: a microscale approach. *Journal of Sea Research*, 41(3), 179-187.
- Sedwick, P.N., Bernhardt, P.W., Mulholland, M.R., Najjar, R.G., Blumen, L.M., Sohst, B.M., Sookhdeo, C., & Widner, B. (2018). Assessing phytoplankton nutritional status and potential impact of wet deposition in seasonally oligotrophic waters of the Mid-Atlantic Bight. *Geophysical Research Letters*, 45(7), 3203-3211.
- Seeberg-Elverfeldt, J., Schlüter, M., Feseker, T., & Kölling, M. (2005). Rhizon sampling of pore waters near the sediment-water interface of aquatic systems. *Limnol. Oceanogr.: Methods*, 3, 361-371.
- Serôdio, J., da Silva, J.M., & Catarino, F. (2001). Use of in vivo chlorophyll a fluorescence to quantify short-term variations in the productive biomass of intertidal microphytobenthos. *Marine Ecology Progress Series*, 218, 45-61.

- Sommer, U. (1999). The impact of herbivore type and grazing pressure on benthic microalgal diversity. *Ecology Letters*, 2(2), 65-69.
- Stewart, S.R., & Berg, R. (2019). National Hurricane Center Tropical Cyclone Report: Hurricane Florence, (AL062018), National Weather Service, National Oceanic and Atmospheric Administration, United States Department of Commerce, Washington, DC.
- Sundbäck, K., Enoksson, V., Granéli, W., & Pettersson, K. (1991). Influence of sublittoral microphytobenthos on the oxygen and nutrient flux between sediment and water: a laboratory continuous-flow study. *Marine Ecology Progress Series*, 263-279.
- Sundbäck, K., Linares, F., Larson, F., Wulff, A., & Engelsen, A. (2004). Benthic nitrogen fluxes along a depth gradient in a microtidal fjord: the role of denitrification and microphytobenthos. *Limnology and Oceanography*, 49(4), 1095-1107.
- Verity, P.G., Yoder, J.A., Bishop, S.S., Nelson, J.R., Craven, D.B., Blanton, J.O., ... & Tronzo, C.R. (1993). Composition, productivity and nutrient chemistry of a coastal ocean planktonic food web. *Continental Shelf Research*, 13(7), 741-776.